Supplementary Figure 1

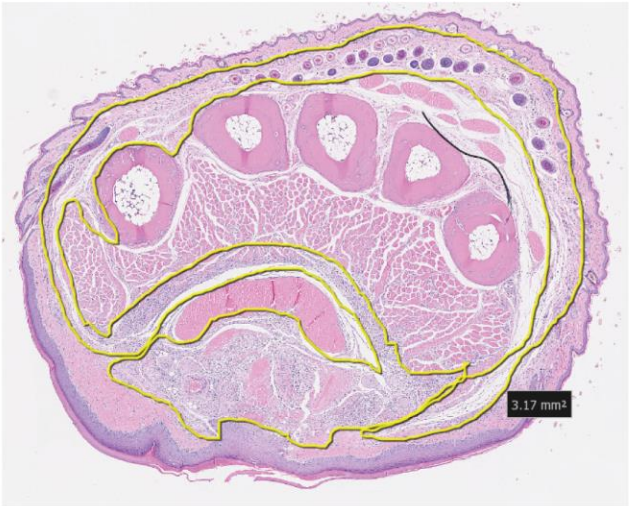

Supplementary Figure 1. Immune cell infiltration area quantification

Example from a WT animal hindpaw at POD4 depicting how the area of immune cell infiltration was quantified. The yellow line indicates the outline of inflammation and the area that was outlined was automatically calculated by NDP.view 2, the area is shown in the black box.

Supplementary Figure 2 **Paw Edema**

Sensory Neuron NLRP3 Knockout

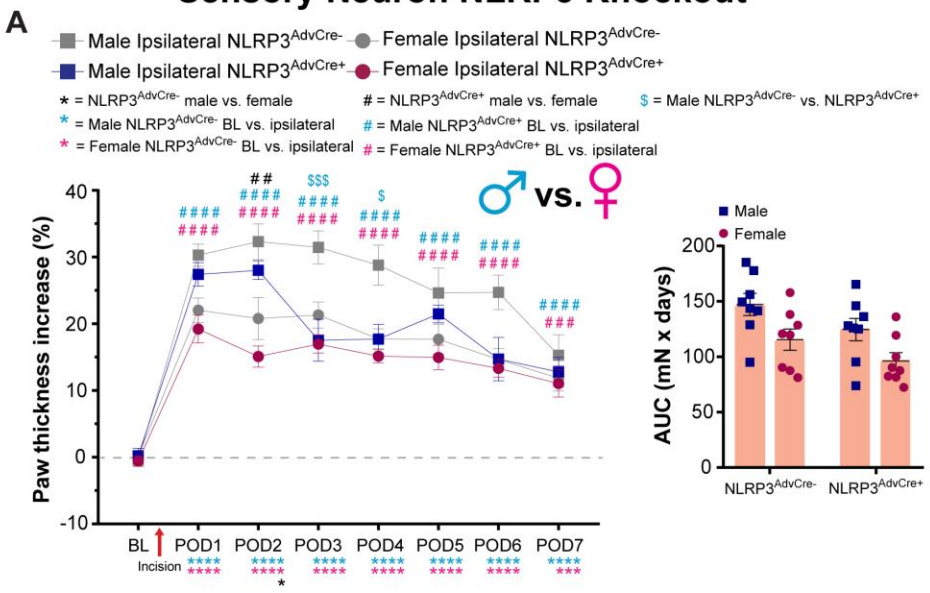

Global NLRP3 Knockout vs. Sensory Neuron NLRP3 Knockout

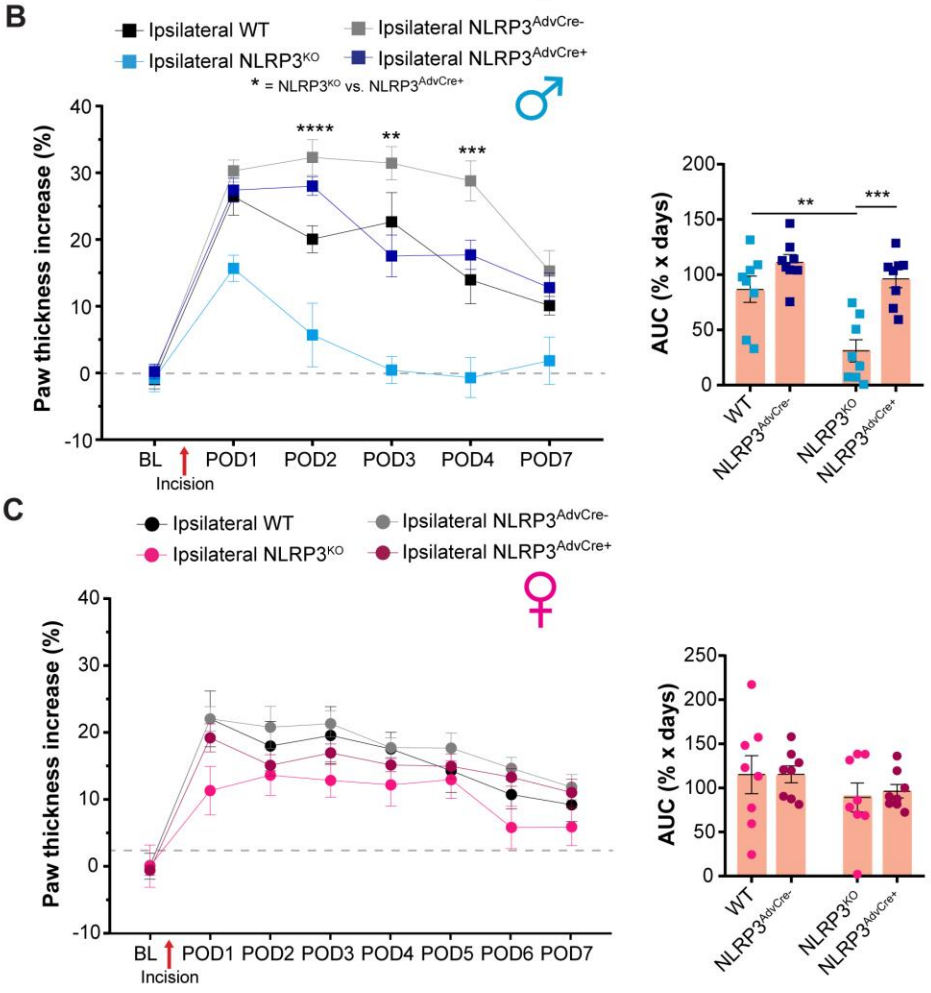

Supplementary Figure 2. Sensory neuron NLRP3 has little effect on paw thickness following incision in male and female mice

(A) Incision induced a significant increase in hindpaw thickness of male NLRP3$^{AdvCre-}$ and NLRP3$^{AdvCre+}$ mice beginning at POD1 and lasting throughout POD7 as compared to baseline (BL). Slight attenuation occurred in NLRP3$^{AdvCre+}$ mice at POD3 and POD4 compared to NLRP3$^{AdvCre-}$ mice. Significantly increased hindpaw thickness was observed in incised female NLRP3$^{AdvCre-}$ and NLRP3$^{AdvCre+}$ mice beginning at POD1 and lasting throughout POD7 as compared to BL. At POD2 NLRP3$^{AdvCre-}$ and NLRP3$^{AdvCre+}$ males appeared to have more edema than NLRP3$^{AdvCre-}$ and NLRP3$^{AdvCre+}$ female mice. Otherwise, male and female NLRP3$^{AdvCre-}$ and NLRP3$^{AdvCre+}$ hindpaw edema did not differ. AUC (normalized to BL) revealed that hindpaw edema of male and female NLRP3$^{AdvCre+}$ mice did not differ. For (A), n= 8 for each genotype, sex, and treatment.

(B) The data from Figure 1A and (A) were used to compare male WT and NLRP3^{KO} mice with male NLRP3$^{AdvCre-}$ and NLRP3$^{AdvCre+}$ mice. Edema following incision was similar in WT and NLRP3$^{AdvCre-}$ mice. Male NLRP3^{KO} and NLRP3$^{AdvCre+}$ mice differed, NLRP3^{KO} mice had significantly less swelling at POD2-POD4 in comparison to NLRP3$^{AdvCre+}$ mice. Differences between WT and NLRP3^{KO} mice and NLRP3$^{AdvCre-}$ and NLRP3$^{AdvCre+}$ mice are shown in Figure 1A and here in (A), respectively. AUC (normalized to BL) confirmed that male NLRP3^{KO} mice had less overall hindpaw edema than NLRP3$^{AdvCre+}$ mice.

(C) The data from Figure 1A and (A) were used to compare female WT and NLRP3^{KO} mice and female NLRP3$^{AdvCre-}$ and NLRP3$^{AdvCre+}$ mice. Female WT and NLRP3$^{AdvCre-}$ mice displayed similar edema following incision. Similarly, the hindpaw swelling was comparable between female NLRP3^{KO} and NLRP3$^{AdvCre+}$ mice. Differences between WT and NLRP3^{KO} mice and NLRP3$^{AdvCre-}$ and NLRP3$^{AdvCre+}$ mice are shown in

Figure 1A and here in (A), respectively. AUC (normalized to BL) confirmed that hindpaw edema in female $NLRP3^{KO}$ mice did not differ from $NLRP3^{AdvCre+}$ mice.

Data shown as mean ± SEM, repeated-measures two-way ANOVA with conservative multiple comparisons and Tukey post hoc test. For (A), black asterisks indicate $NLRP3^{AdvCre-}$ male versus female, blue asterisks indicate male $NLRP3^{AdvCre-}$ BL versus ipsilateral, pink asterisks indicate female $NLRP3^{AdvCre-}$ BL versus ipsilateral, black pound sign indicates $NLRP3^{AdvCre+}$ male versus female, blue pound sign indicates $NLRP3^{AdvCre+}$male BL versus ipsilateral, pink pound sign indicates $NLRP3^{AdvCre+}$ female BL versus ipsilateral, and blue dollar sign indicates male $NLRP3^{AdvCre+}$ versus $NLRP3^{AdvCre-}$: *$p < 0.05$, ***$p < 0.001$, ****$p < 0.0001$ WT BL versus ipsilateral or male versus female; $^{\#\#}p < 0.01$, $^{\#\#\#}p < 0.001$, $^{\#\#\#\#}p < 0.0001$ $NLRP3^{KO}$ BL versus ipsilateral or male versus female; $^{\$}p < 0.05$, $^{\$\$\$}p < 0.001$ male $NLRP3^{AdvCre+}$ versus $NLRP3^{AdvCre-}$. For (B), **$p < 0.01$, ***$p < 0.001$, ****$p < 0.0001$ $NLRP3^{KO}$ versus $NLRP3^{AdvCre+}$. For (A), (B), and (C), AUC: **$p < 0.01$, ***$p < 0.001$ (two-way ANOVA and Sidak post hoc test) and dashed line represents average baseline (BL) values.

Supplementary Figure 3

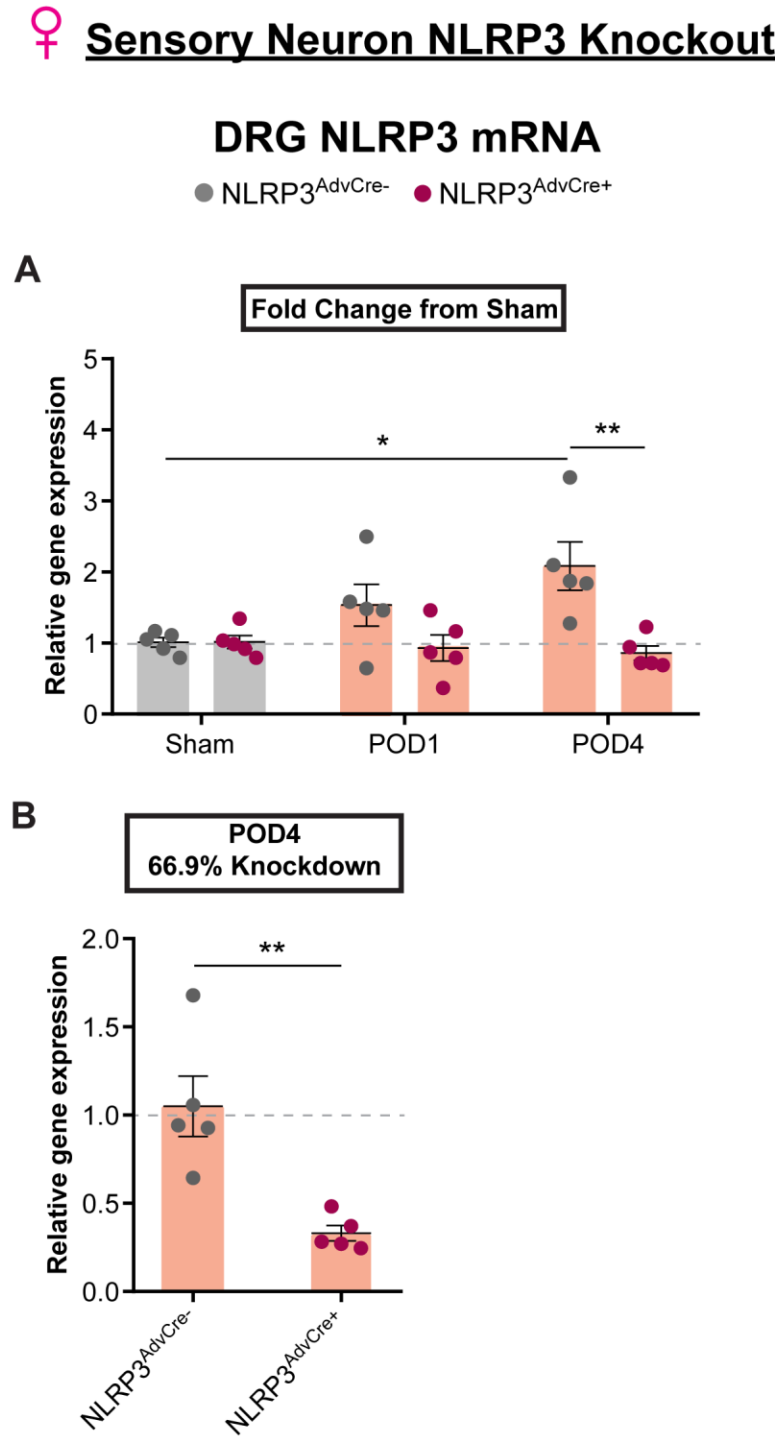

Supplementary Figure 3. NLRP3$^{AdvCre+}$ mice have a 66.9% knockdown of NLRP3 in sensory neurons

(A) qPCR of whole DRG normalized to GAPDH and sham mRNA levels. Surgical incision induced a significant increase in NLRP3 relative gene expression at POD4 in NLRP3$^{AdvCre-}$ DRG compared to sham and NLRP3$^{AdvCre+}$ samples from females. For (A), n = 5 for each treatment and genotype.

(B) POD4 was used to determine the percent knockdown of NLRP3 since NLRP3 was significantly upregulated at POD4 in comparison to sham controls in (A). NLRP3$^{AdvCre+}$ DRG had 66.9% less NLRP3 than NLRP3$^{AdvCre-}$ DRG at POD4.

Data shown as mean ± SEM. For (A), *$p < 0.05$, **$p < 0.01$ (two-way ANOVA and Tukey post hoc test), dashed line represents sham levels normalized to 1. For (B), **$p < 0.01$ (unpaired t-test), dashed line represents NLRP3$^{AdvCre-}$ levels normalized to 1.

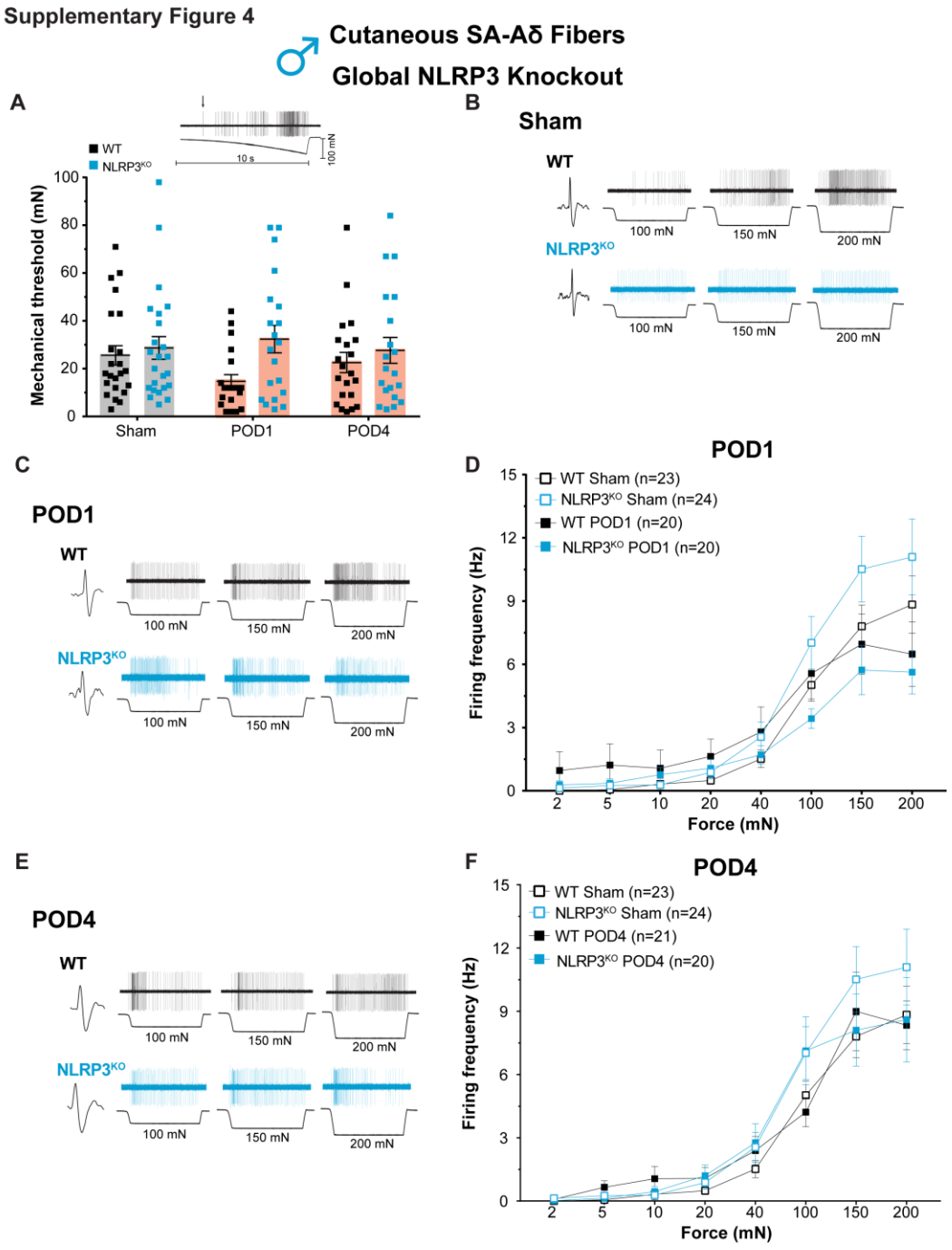

Supplementary Figure 4. SA-Aδ mechanical firing is not affected by incision or deletion of NLRP3

(A) Representative trace of mechanical threshold ramp stimulus. Arrow designates mechanical threshold. Tibial skin-nerve preparations from male WT and NLRP3^{KO} mice were used to determine Aδ

fiber mechanical threshold. Incision had no effect on mechanical thresholds of WT or NLRP3^{KO} Aδ fibers at POD1 and POD4 compared to sham controls.

(B, C, E) Example Aδ traces of mechanically-evoked action potentials in response to 100, 150, and 200 mN 10 s square wave mechanical stimuli from WT (top) and NLRP3^{KO} (bottom) preparations. (B) Sham traces, (C) POD1 traces, and (E) POD4 traces.

(D) The firing frequency in response to incremental mechanical stimulation of Aδ fibers from WT and NLRP3^{KO} mice was unaffected by incision at POD1.

(F) Aδ fiber mechanical firing frequency was unchanged by incision at POD4 in preparations from WT and NLRP3^{KO} in comparison to sham controls.

For (A), (D), and (F); WT: sham n= 7 and 23 fibers, POD1 n= 7 and 20 fibers, POD4 n= 6 and 21 fibers. NLRP3^{KO}: sham n= 8 and 24 fibers, POD1 n= 5 and 20 fibers, POD4 n= 6 and 20 fibers.

Data shown as mean ± SEM. The sham groups in (D) and (F) are the same data but were separated for clarity and statistics were run on all groups together (sham, POD1, and POD4) where POD1 and POD4 were considered as different groups. For (A), ordinary two-way ANOVA and Tukey post hoc test. For (D) and (F), repeated measures mixed-model test with a Sidak post hoc test.

Supplementary Figure 5

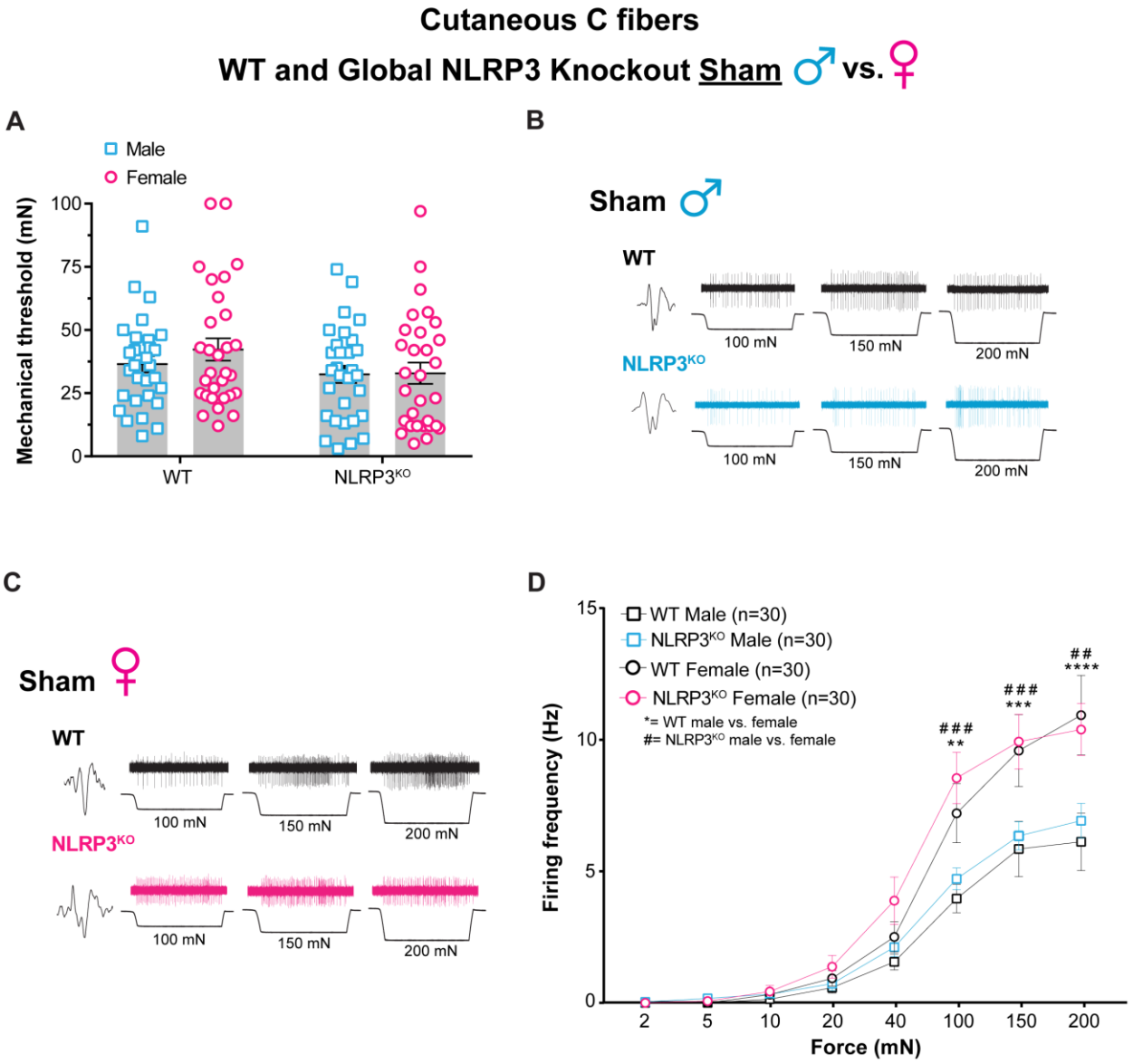

Supplementary Figure 5. Uninjured female nociceptor terminals display higher firing frequencies in response to high forces than males

(A) The data is from sham male and female preparations in Figures 7 and 8. The mechanical thresholds of male and female NLRP3^{KO} preparations were similar.

(B, C) Representative traces of evoked C fiber action potentials in response to 100, 150, and 200 mN 10 s square wave mechanical stimuli from WT (top) and NLRP3^{KO} (bottom) preparations (traces from Figures 7 and 8). (B) Male traces and (C) female traces.

(D) The data is from sham male and female preparations in Figures 7 and 8. The firing frequencies of C fibers in response to incremental increases in mechanical stimuli were higher from 100-200 mN in female WT and NLRP3^{KO} preparations compared to male WT and NLRP3^{KO} preparations.

Data shown as mean ± SEM. For (A), ordinary two-way ANOVA and Tukey post hoc test. For (D), repeated measures mixed-model analysis with a Sidak post hoc test.

Supplementary Figure 6

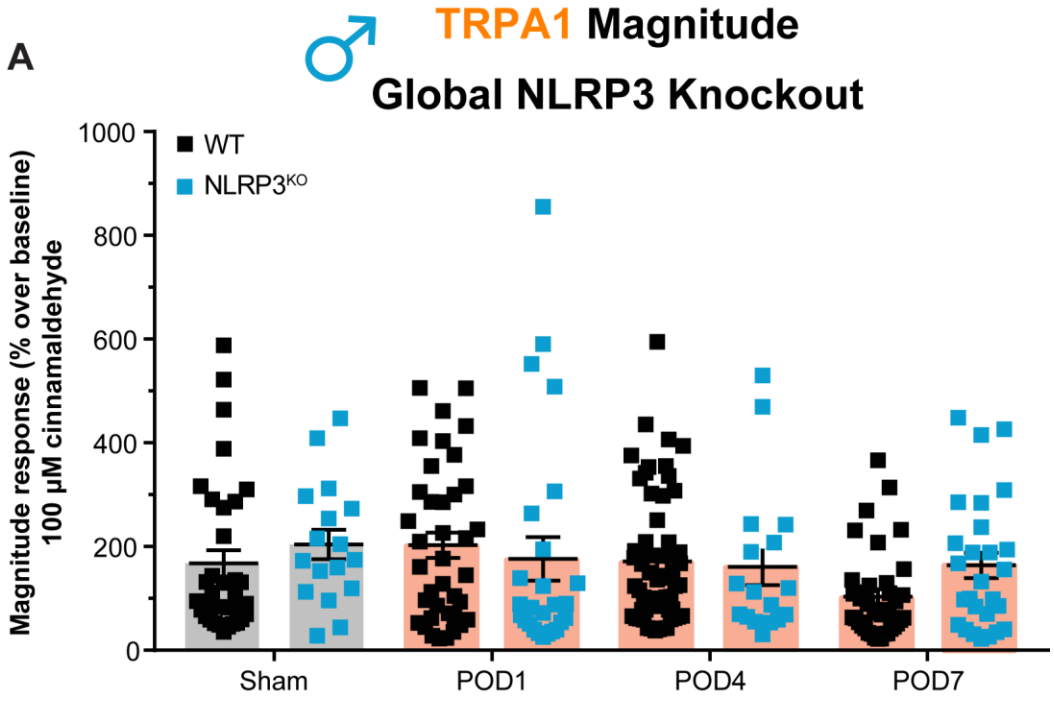

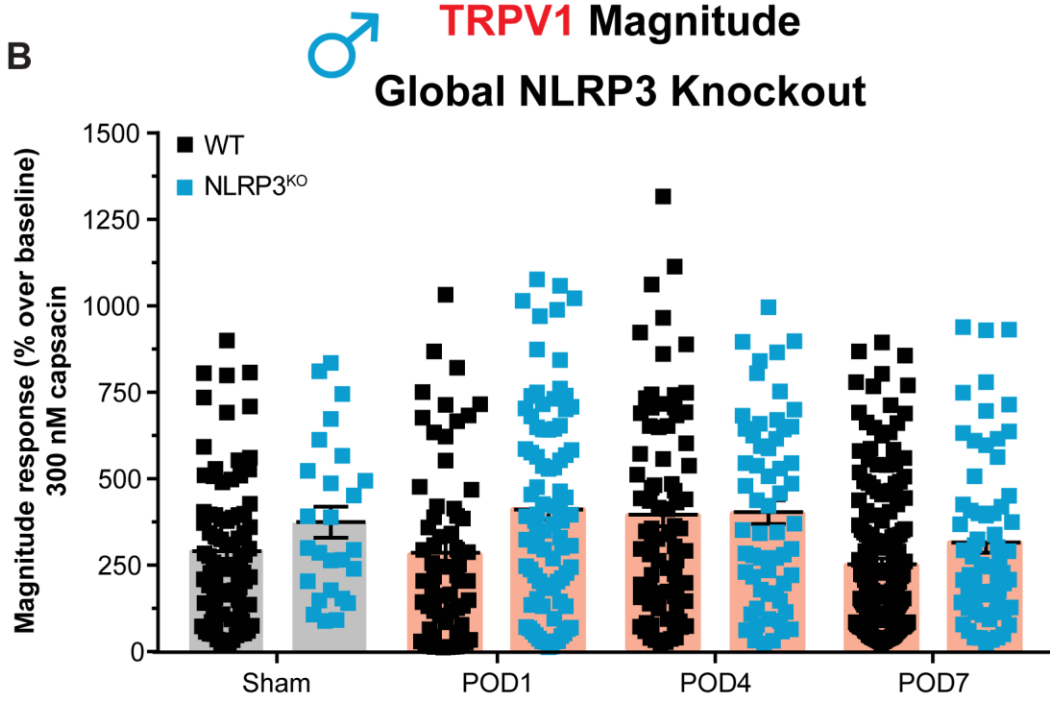

Supplementary Figure 6. Deletion of NLRP3 and incision do not change TRPA1 and TRPV1 magnitude in response to agonist application

(A) Magnitude in response to application of TRPA1 agonist cinnamaldehyde to DRG somata did not change after incision in either WT or $NLRP3^{KO}$ neurons.

(B) WT and $NLRP3^{KO}$ DRG neuron magnitude response to capsaicin, a TRPV1 agonist, was not affected by incision.

Data shown as mean ± SEM, two-way ANOVA and Sidak post hoc test.